Infragravity-Frequency (0.005–0.05 Hz) Motions on the Shelf. Part I: Forced Waves

T. H. C. HERBERS*

Center for Coastal Studies, Scripps Institution of Oceanography, La Jolla, California

STEVE ELGAR

Electrical Engineering and Computer Science, Washington State University, Pullman, Washington

R. T. GUZA

Center for Coastal Studies, Scripps Institution of Oceanography, La Jolla, California

(Manuscript received 27 September 1992, in final form 23 April 1993)

ABSTRACT

This is Part 1 of a two-part study of infragravity-frequency (nominally 0.005–0.05 Hz) motions on the continental shelf. Data from a large aperture (250 m × 250 m) array of 24 bottom-mounted pressure transducers deployed in 13 m depth is used to investigate the local forcing of infragravity motions by nonlinear difference-frequency interactions of surface gravity waves. Second-order nonlinear theory (Hasselmann) and observed swell–sea frequency–directional spectra are used to predict the energy levels of forced infragravity waves. For a wide range of wave conditions, the predicted forced wave levels are lower than the observed energy levels, suggesting that the infragravity band contains a mix of free and forced waves. Bispectral analysis is used to estimate the relative amounts of free and forced infragravity energy. Good agreement between bispectrum-based estimates and theoretical predictions of forced wave energy confirms that second-order nonlinear theory accurately predicts locally forced infragravity motions. The contribution of forced waves to the total infragravity energy, ranging from less than 0.1% to about 30%, is largest when the infragravity energy is maximum, consistent with previously noted trends in similar water depths. The bispectral technique developed here to estimate the energy of forced and free infragravity waves is used in Part 2 to investigate, with data from single-point pressure gauges, the shelfwide variability of free infragravity energy.

1. Introduction

Ocean surface gravity waves are most energetic in the swell–sea frequency band, typically 0.06–0.3 Hz. Lower-frequency motions in the so-called infragravity band (nominally 0.005–0.05 Hz) are generally weak in the deep ocean (the bottom pressure variance is at most a few centimeters squared, Webb et al. 1991) but can be very energetic in shallow water (variances > 100 and 1000 cm^2 in 10 m depth and at the shoreline, respectively, Wright et al. 1982; Guza and Thornton 1985; Okihiro et al. 1992; Elgar et al. 1992). Although field observations have shown that infragravity energy levels are highly correlated with swell-sea energy (e.g., Munk 1949; Tucker 1950; Holman et al. 1978, among others), the generation of infragravity motions is not well understood. Nonlinear interaction of two surface waves theoretically excites a forced secondary wave with the difference-frequency Δf (e.g., Longuet-Higgins and Stewart 1962; Hasselmann 1962), and the theoretically expected phase-coupling between swell-sea and difference-frequency infragravity motions has been detected in field observations (e.g., Hasselmann et al. 1963; Elgar and Guza 1985; Okihiro et al. 1992; Elgar et al. 1992). However, although qualitative theoretical predictions of the forced infragravity spectrum $E_{\text{forced}}(\Delta f)$ are roughly consistent with the observed spectrum $E(\Delta f)$ when surface waves are very energetic (Sand 1982), the predicted $E_{\text{forced}}(\Delta f)$ accounts for only a small fraction of $E(\Delta f)$ when swell-sea (and infragravity) energy is low (Okihiro et al. 1992). The accuracy of $E_{\text{forced}}(\Delta f)$ predictions in these studies was limited by either the assumption of unidirectional swell-sea (Sand 1982) or the low resolution of pitch and roll-type measurement systems (Okihiro et al. 1992).

Motions other than locally forced secondary waves are clearly important at infragravity frequencies. Observed alongshore wavenumber spectra (Munk et al. 1964; Huntley et al. 1981; Oltman-Shay and Guza 1987; Howd et al. 1991; Oltman-Shay 1991, personal communication), weak energy levels in the deep ocean

* Current affiliation: Department of Oceanography, Naval Postgraduate School, Monterey, California.

Corresponding author address: Dr. Thomas H. C. Herbers, Code OC/He, Naval Postgraduate School, Monterey, CA 93943-5000.

(Webb et al. 1991), and cross-shelf energy variations (Okihiro et al. 1992; Elgar et al. 1992) all suggest that the "other" infragravity energy consists predominantly of free surface gravity waves refractively trapped on the shelf with only weak radiation to the deep ocean. Various qualitative models suggest that these free waves are generated through nonlinear interactions and/or breaking processes close to shore (e.g., Longuet-Higgins and Stewart 1962; Gallagher 1971; Bowen and Guza 1978; Foda and Mei 1981; Symonds et al. 1982; Mei and Benmoussa 1984; Schäffer and Svendsen 1988; Schäffer et al. 1990; List 1992).

This is Part 1 of a two-part study of infragravity-frequency motions on the continental shelf. Pressure array data acquired in 13 m depth are used to quantitatively verify second-order nonlinear theory (Hasselmann 1962) for the local forcing of infragravity motions by swell and sea. The field experiment and data reduction are described in section 2. In section 3, comparisons of the predicted $E_{\text{forced}}(\Delta f)$ and the observed $E(\Delta f)$ show that (similar to past studies) $E_{\text{forced}}(\Delta f)$ is always less (and in many cases much less) than $E(\Delta f)$. Nonlinear theory is not verified by these comparisons. In section 4, integrals of the bispectrum are used to estimate the energy levels of free and forced infragravity waves. The observed forced (i.e., phase coupled to swell–sea) infragravity energy levels agree well with theoretical predictions. Sources of errors in the results are discussed in section 5. The bispectral technique developed here is used in Part 2 to investigate, with data from single-point pressure gauges, the variation of free infragravity energy as a function of wave conditions, water depth, and geographic setting.

2. Field experiment and data reduction

An array of 24 pressure sensors was deployed for 9 months on the seafloor in 13 m depth, 2 km offshore of the U.S. Army Corps of Engineers Field Research Facility at Duck, North Carolina. The field site, a sandy beach along a relatively straight barrier island with no nearby headlands, is exposed to ocean waves from a wide range (about 180°) of propagation directions (Fig. 1a). Repeated high-resolution bathymetric surveys using a towed sled with surface piercing optical targets and a shore-based laser positioning system show that the seafloor at the array location is featureless in the alongshore direction, with a mean cross-shore slope of about 0.005 (Birkemeier et al. 1991). Small depth variations (<1 m) across the array, which spans about 250 m in both the cross-shore and alongshore directions (Fig. 1b), are neglected in this study. The relative positions of the sensors were accurately known. Extensive triangulation by scuba divers using highly tensioned wires between many sensor pairs reduced uncertainties in the sensor locations to less than about 1% of the distance from the array center. To reduce flow noise the pressure sensors were buried about 10 cm within the seabed.

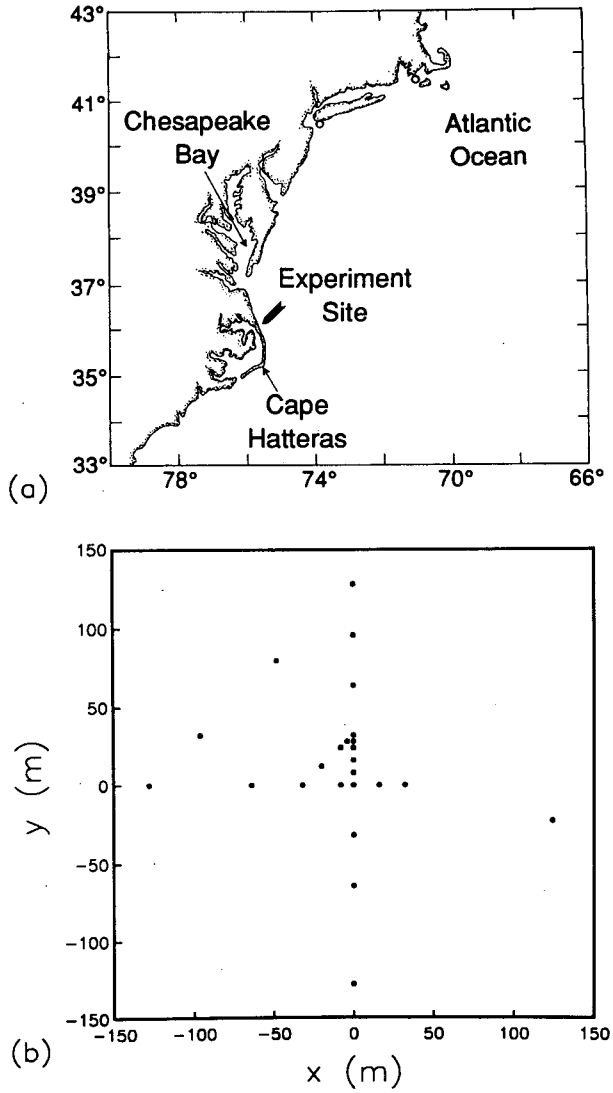

FIG. 1. Pressure sensor array location (a) and plan view (b). The positive x axis is directed offshore.

Fifteen data runs, each 2 h and 50 min long and collected at a 4-Hz sample rate, were selected for analysis. The data span a wide range (0.3–3.3 m) of significant wave heights (defined as $4E_\eta^{1/2}$ with E_η the surface elevation variance in the frequency range 0.06–0.24 Hz, estimated from the bottom pressure data with a linear theory depth correction). Mean frequencies (of the surface elevation energy in the same frequency range) varied between 0.10 and 0.17 Hz. Estimates of spectra, bispectra, and cross-spectra were obtained from Fourier transforms of overlapped, detided, and tapered 34-minute data segments, through a combination of ensemble averaging and frequency band merging. Spectral and bispectral estimates were further stabilized by spatial averaging over three array elements separated by about 200 m.

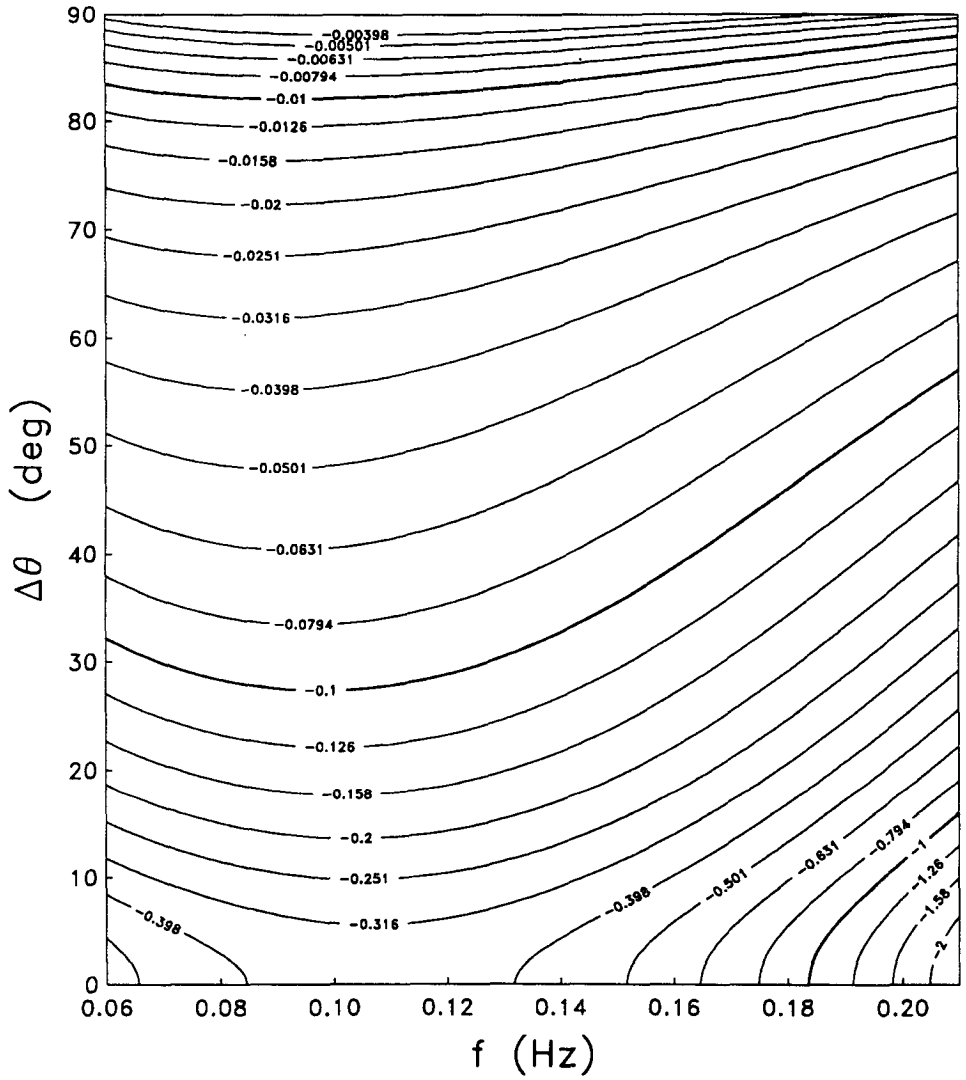

FIG. 2. The dependence of the interaction coefficient D [Eqs. (1) and (A5), contours at $10^{0.1}$ intervals in units m^{-1}] in 13 m depth on f and $\Delta\theta$, for a fixed $\Delta f = 0.03$ Hz. Two primary (swell–sea) waves (frequencies f, $f + \Delta f$, and directional difference $\Delta\theta$) force a secondary (infragravity) wave with frequency Δf.

3. Predictions of forced waves

A perturbation expansion in weak nonlinearity shows that the interaction between two surface gravity waves with slightly different frequencies f and $f + \Delta f$ excites a forced secondary wave with the difference frequency Δf (e.g., Longuet-Higgins and Stewart 1962; Hasselmann 1962). The spectrum $E_{\text{forced}}(\Delta f)$ of secondary pressure at the seafloor is [Hasselmann 1962; Hasselmann et al. 1963; see Eq. (A8) of the Appendix, neglecting interactions involving primary waves with frequency $< \Delta f$]

$$E_{\text{forced}}(\Delta f) = 2\int_{\Delta f}^{\infty} df \int_0^{2\pi} d\theta_1 \int_0^{2\pi} d\theta_2 D^2(f + \Delta f, -f, \Delta\theta + \pi) E(f + \Delta f, \theta_1) E(f, \theta_2),$$

where $E(f, \theta)$ is the frequency–directional spectrum of primary (swell and sea) seafloor pressure, $D(f + \Delta f, -f, \Delta\theta + \pi)$ is the difference-interaction coefficient for two primary waves with frequencies f and $f + \Delta f$ and a difference $\Delta\theta$ ($= |\theta_1 - \theta_2|$) in propagation direction [Eq. (A5) of the Appendix]. Okihiro et al. (1992) discuss the dependence of D on the primary wave properties and water depth. In 13 m depth, D is significantly reduced by directional spreading. For a value of $\Delta\theta = 30°$ (typical for the data discussed here), D is about 25% of the maximum value for colinear ($\Delta\theta = 0$) primary waves and $E_{\text{forced}}(\Delta f)$ is reduced by more than an order of magnitude (Fig. 2). Accurate estimates of $E(f, \theta)$ were not available in previous studies. For the dominant swell and sea (0.06 Hz $< f <$ 0.24 Hz; ex-

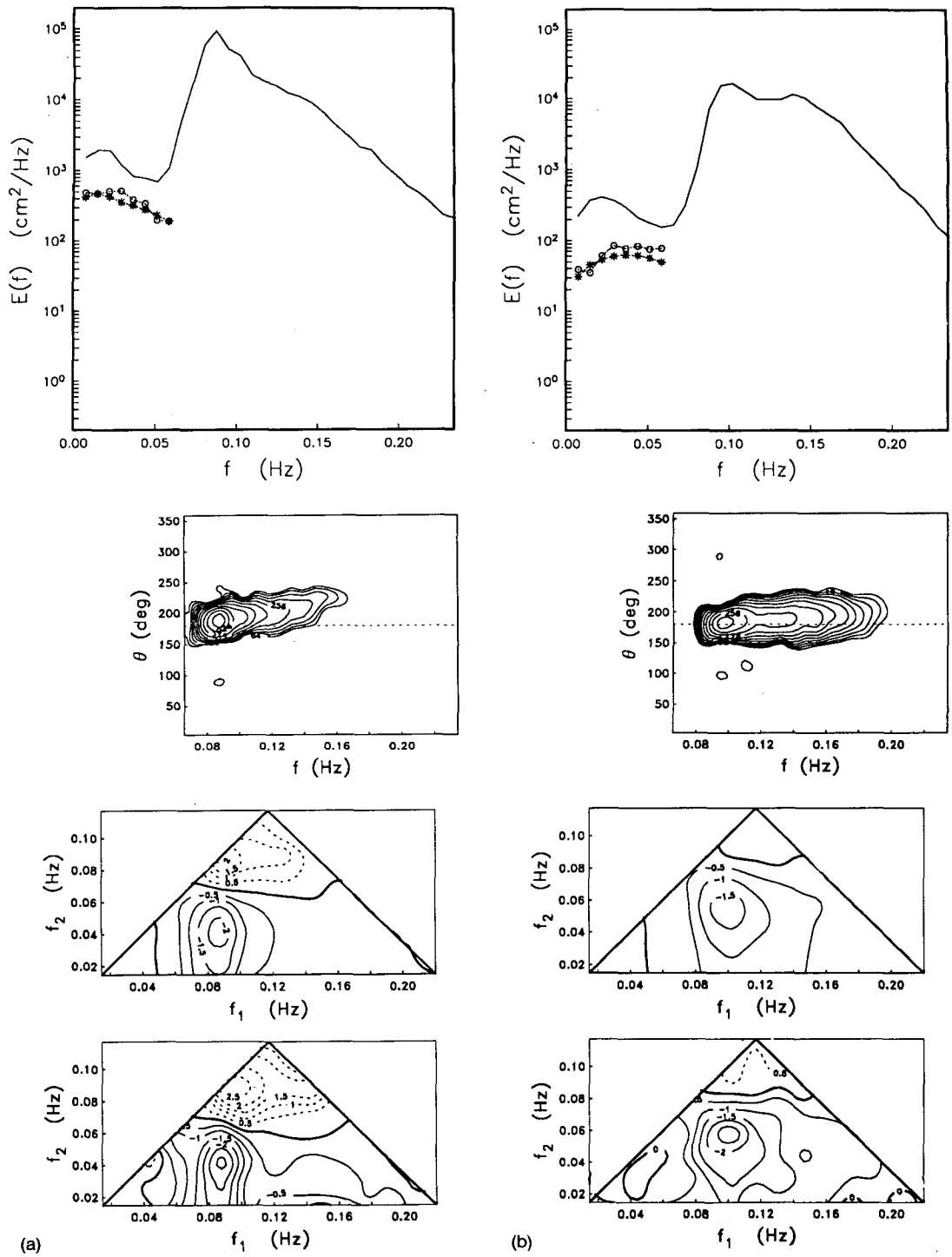

FIG. 3. Top panels: Observed bottom pressure spectra $E(f)$ (solid curves), and predicted [asterisks, Eq. (1)] and observed [circles, Eq. (6)] forced infragravity wave spectra $E_{\text{forced}}(\Delta f)$. Upper-middle panels: observed frequency-directional spectra of seafloor pressure $E(f, \theta)$ at swell–sea frequencies (contours at $2^{0.5}$ intervals in units cm^2/Hz^0). Normal incidence to the beach is $\theta = 180°$. Lower-middle and bottom panels: predicted [Eqs. (A11), (4)] and observed [real part of Eqs. (2), (4)] normalized bispectra $b(f_1, f_2)$, respectively (contours at 0.5 $\text{Hz}^{-1/2}$ intervals). The observation dates, total swell–sea energies, and infragravity energies are, respectively, (a) 26 October 1990, 6993 cm^2, 66 cm^2; (b) 19 May 1991, 3785 cm^2, 15 cm^2; and (c) 23 December 1990, 769 cm^2, 5 cm^2. The frequency resolution of the estimates is 0.007 Hz for $E(f)$, $E_{\text{forced}}(\Delta f)$, and $E(f, \theta)$, and 0.014 Hz for $b(f_1, f_2)$.

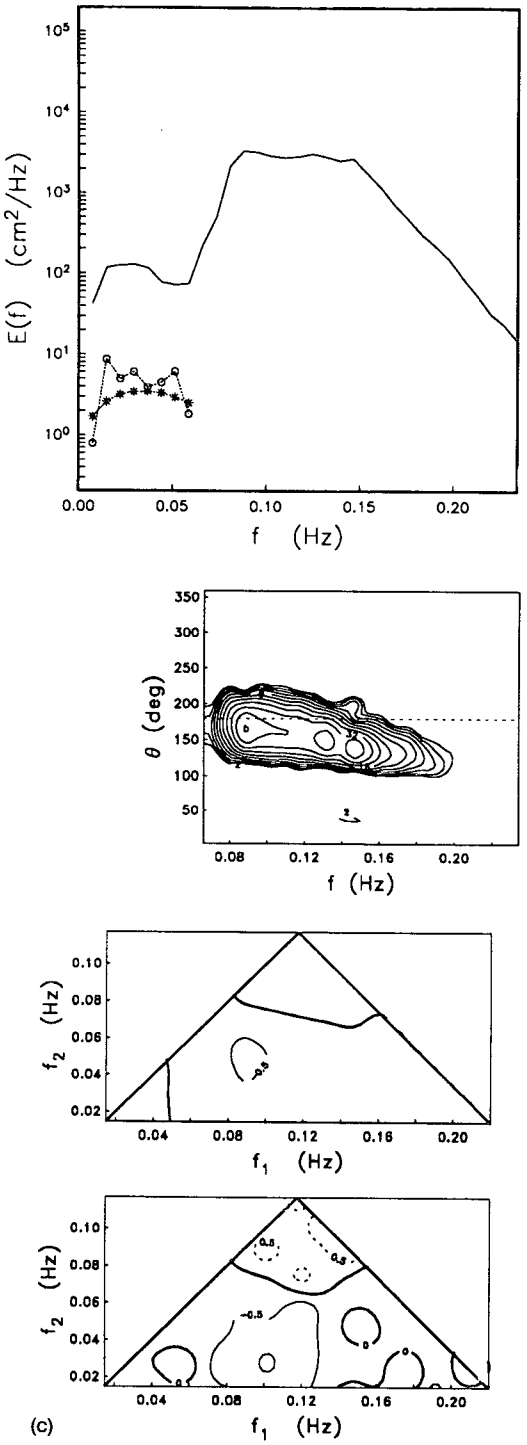

FIG. 3. (*Continued*)

amples are shown in Fig. 3) $E(f, \theta)$ were estimated from the array measurements (Fig. 1b) with a variational technique (Herbers and Guza 1990). Predictions of $E_{\text{forced}}(\Delta f)$ were obtained by substituting the observed $E(f, \theta)$ and the theoretical interaction coefficient D in Eq. (1). Errors in $E_{\text{forced}}(\Delta f)$ predictions resulting from the exclusion of primary waves with $f < 0.06$ Hz and $f > 0.24$ Hz are expected to be small. Although D^2 is maximum for colinear high-frequency primary waves (Fig. 2), infragravity forcing by locally generated seas is negligible because bottom pressure spectral levels at frequencies > 0.2 Hz are much lower (even during the initial stages of wind wave generation) than the energy levels of everpresent (at the exposed Duck field site) lower-frequency swells (e.g., Fig. 3, top panels). Wave fields dominated by swell with frequencies < 0.06 Hz are rare at the Duck field site and not considered here.

Predictions of $E_{\text{forced}}(\Delta f)$ are compared to the observed infragravity spectrum $E(\Delta f)$ in the top panels of Figs. 3a–c for wave fields with high, moderate, and low swell–sea energy, respectively. Predicted and observed spectral levels are compared for all 15 runs and all frequencies in the infragravity band $0.005 < \Delta f < 0.05$ Hz in Fig. 4a. Integrated (over the infragravity frequency band), predicted ($\int d\Delta f E_{\text{forced}}(\Delta f)$), and observed ($\int d\Delta f E(\Delta f)$) infragravity energies are compared in Fig. 4b. The observed frequency-integrated infragravity energy varies between 0.5 and 66 cm^2, and is between 3 and 1500 times larger than the predicted forced infragravity energy. The greatest differences occur when the swell-sea and infragravity energies are smallest, similar to previous results at different sites [i.e., compare the present Fig. 4b to Fig. 7a,b in Okihiro et al. (1992)]. These energy comparisons do not verify second-order nonlinear theory because the locally forced waves are apparently submerged in a background of free (i.e., not locally forced) infragravity motions.

4. Observations of forced waves

Bispectral analysis (Hasselmann et al. 1963) is used to isolate the forced wave component of the infragravity motions. Analogous to the (second-order) energy density spectrum $E(f)$,

$$E(f)df \equiv 2\mathbf{E}\{dP(f)dP(-f)\}, \qquad (2a)$$

the (third-order) bispectrum $B(f_1, f_2)$ is defined as

$$B(f_1, f_2)df_1 df_2 \equiv 2\mathbf{E}\{dP(f_1)dP(f_2)dP(-f_1 - f_2)\}, \qquad (2b)$$

where $\mathbf{E}\{\ \}$ denotes the expected value and $dP(f)$ is the Fourier–Stieltjes representation of the pressure time series $p(t)$,

$$p(t) = \int_{-\infty}^{\infty} dP(f) \exp(2\pi i f t); \qquad (3)$$

$B(f_1, f_2)$ vanishes for a linear (Gaussian) wave field. Nonzero $B(f_1, f_2)$ results from phase-coupled triads consisting of two primary waves and a forced secondary wave with frequencies f_1, f_2, and $f_1 + f_2$ [Hasselmann

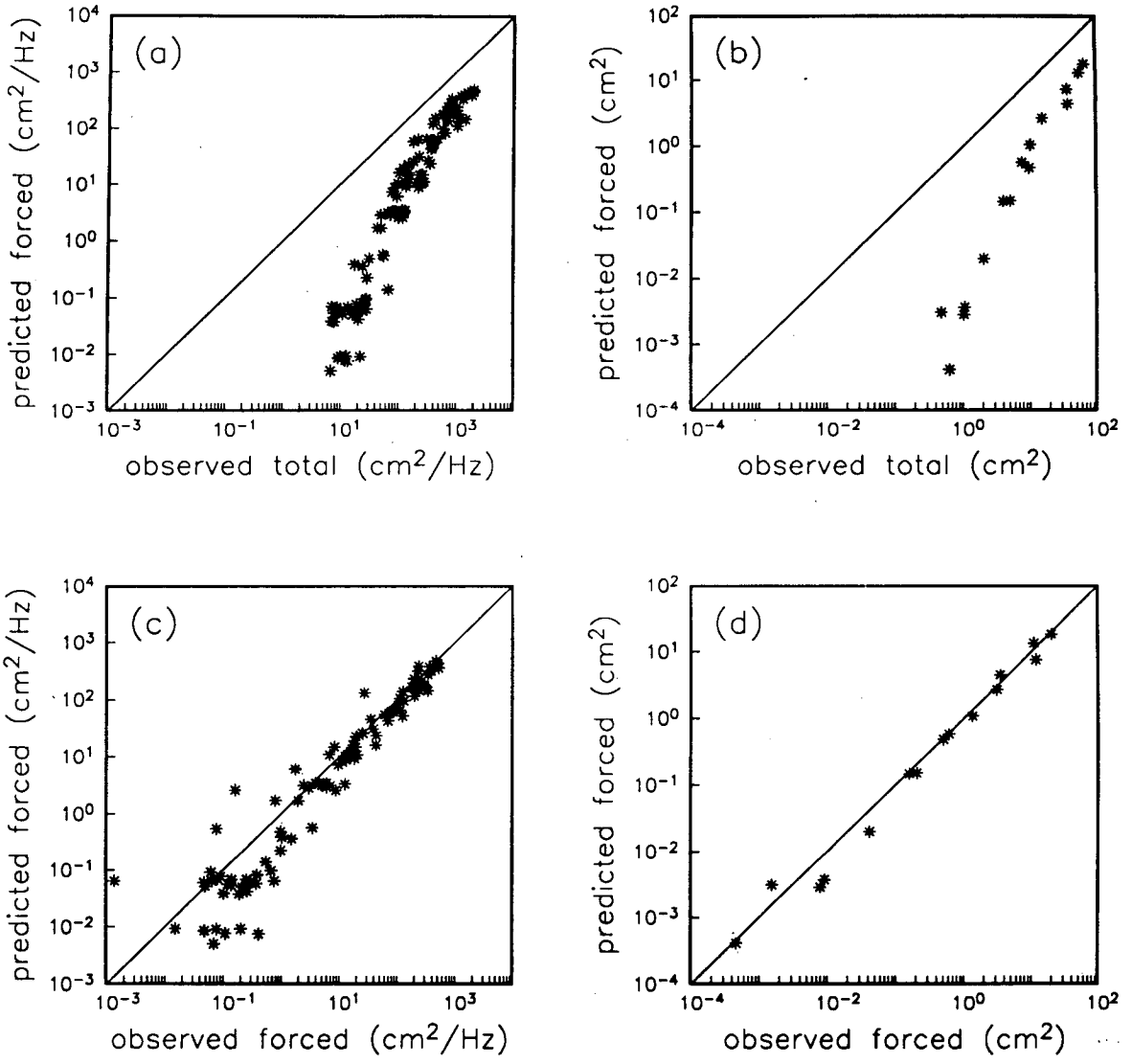

FIG. 4. For all 15 runs. (a) Predicted forced [$E_{\text{forced}}(\Delta f)$, Eq. (1)] versus observed total [$E(\Delta f)$] energy density at infragravity frequencies Δf in the range 0.005–0.05 Hz. (b) Predicted forced [$\int_{0.005\text{ Hz}}^{0.05\text{ Hz}} d\Delta f E_{\text{forced}}(\Delta f)$, Eq. (1)] versus observed total [$\int_{0.005\text{ Hz}}^{0.05\text{ Hz}} d\Delta f E(\Delta f)$] frequency-integrated infragravity energy. (c) Predicted [Eq. (1)] versus observed [based on bispectral analysis, Eq. (6)] forced infragravity energy density [$E_{\text{forced}}(\Delta f)$] at frequencies Δf in the range 0.005–0.05 Hz. (d) Predicted [Eq. (1)] versus observed [based on bispectral analysis, Eq. (10)] frequency-integrated forced infragravity energy [$\int_{0.005\text{ Hz}}^{0.05\text{ Hz}} d\Delta f E_{\text{forced}}(\Delta f)$].

et al. 1963; Eqs. (A9)–(A11) of the Appendix]. Sum and difference interactions between primary swell–sea components with frequencies f and $f + \Delta f$ contribute to $B(f + \Delta f, f)$ and $B(f, \Delta f)$, respectively. A relative measure $b(f_1, f_2)$ of nonlinear phase coupling between components with frequencies f_1, f_2, and $f_1 + f_2$ is obtained by normalizing $B(f_1, f_2)$ by the spectral densities at the three interacting frequencies (Haubrich 1965; but with a slightly different normalization)

$$b(f_1, f_2) \equiv \frac{B(f_1, f_2)}{[E(f_1)E(f_2)E(f_1 + f_2)]^{1/2}}. \quad (4)$$

The observed [Eq. (4)] and predicted [Eq. (A11) using the observed swell–sea $E(f, \theta)$] $b(f_1, f_2)$ are qualitatively similar (Fig. 3). Note that the observed and predicted bispectra include both sum and difference interactions, and are normalized by the same (observed) spectral densities [Eq. (4)]. The imaginary part of $b(f_1, f_2)$ (not shown in Fig. 3) theoretically vanishes [Eq. (A11)], and the approximately random scatter about zero of the observed imaginary part (shown in Fig. 5a for all runs) illustrates the considerable statistical uncertainty in these bispectral estimates. When swell–sea energy levels are high (26 October, Fig. 3a), non-

linearities are relatively strong and the real part of $b(f_1, f_2)$ is nonzero over a wide range of frequencies. Difference-frequency interactions dominate the predicted negative values of $b(f_1, f_2)$ for f_1 close to the spectral peak frequency ($f_1 \approx 0.09$ Hz) and f_2 ($=\Delta f$) in the infragravity band ($f_2 < 0.05$ Hz). The positive $b(f_1, f_2)$ for f_1 and f_2 both close to the spectral peak frequency indicate sum-frequency interactions [discussed in more detail in Herbers and Guza (1994)]. For moderate swell–sea energy (19 May, Fig. 3b) similar negative bispectral levels are both predicted and observed (i.e., for $f_1 \approx 0.1$ Hz, $f_2 \leq 0.07$ Hz). However, unlike the twice as energetic 26 October wave field, free wind-generated seas dominate the seafloor pressure spectrum at double swell frequencies, and sum frequency interactions are not significant [i.e., $b(f_1, f_2)$ is small for f_1, f_2 close to the 0.1 Hz swell peak]. For a low energy wave field (23 December, Fig. 3c) the observed and predicted $b(f_1, f_2)$ are small at all f_1, f_2, with the predicted $E_{\text{forced}}(\Delta f)$ about 10^2 lower than the observed infragravity energy levels. Free wave motions dominate the bottom-pressure spectrum, and relatively weak forced waves cannot be detected owing to the statistical uncertainty in the $b(f_1, f_2)$ estimates [Fig. 5a, the statistical scatter in the theoretically zero imaginary part indicates that the minimum detectable $b(f_1, f_2)$ level is about 0.5 $\text{Hz}^{-1/2}$].

The forced wave spectral density $E_{\text{forced}}(\Delta f)$ can be estimated by integrating the bispectrum $B(f, \Delta f)$ over all wave pairs with difference-frequency Δf

$$b_i(\Delta f) \equiv \frac{2\int_{\Delta f}^{\infty} df B(f, \Delta f)}{\left[2\int_{\Delta f}^{\infty} df E(f+\Delta f)E(f)E(\Delta f)\right]^{1/2}}. \tag{5}$$

Substitution of the theoretical expression for B, Eq. (A11) in Eq. (5), and neglecting the contributions of interactions involving infragravity-frequency primary waves, yields

$$\frac{E_{\text{forced}}(\Delta f)}{E(\Delta f)} = \alpha_i(\Delta f)|b_i(\Delta f)|^2, \tag{6}$$

where

$$\alpha_i(\Delta f) = \frac{M_2(\Delta f)}{M_1^2(\Delta f)} \tag{7}$$

with

$$M_n(\Delta f) = \frac{\int_{\Delta f}^{\infty} df \int_0^{2\pi} d\theta_1 \int_0^{2\pi} d\theta_2 D^n(f+\Delta f, -f, \Delta\theta+\pi)E(f+\Delta f, \theta_1)E(f, \theta_2)}{\int_{\Delta f}^{\infty} df \int_0^{2\pi} d\theta_1 \int_0^{2\pi} d\theta_2\, E(f+\Delta f, \theta_1)E(f, \theta_2)}. \tag{8}$$

Hence, the fraction of the energy density at frequency Δf that is locally, nonlinearly forced is approximately given by $|b_i(\Delta f)|^2$, with a negative bias [i.e., $\alpha_i > 1$, Eqs. (6)–(8)] owing to variations in the interaction coefficient D over contributing wave triads. This bias is small for the $E(f, \theta)$ typically observed in coastal environments (see section 5). Thus, forced wave spectra can be estimated from observations with a single pressure sensor [Eq. (6), setting α_i equal to 1]. The observed [Eqs. (2), (5), (6), with $f + \Delta f = 0.24$ Hz the upper limit of integration] and theoretically predicted [Eq. (1), also with 0.24 Hz as an upper limit] $E_{\text{forced}}(\Delta f)$ are generally in good agreement, as illustrated for the three example cases in Fig. 3 (cf. circles and asterisks in the upper panels), and as shown for all runs in Fig. 4c. The observed negative real and small imaginary parts of $b_i(\Delta f)$ (Fig. 5b) are consistent with theory.

The contribution of forced waves to the total infragravity energy in the frequency range $[\Delta f_{\min}, \Delta f_{\max}]$ can be obtained by double integration of the bispectrum over all difference-frequency interactions

$$b_{ii} \equiv \frac{2\int_{\Delta f_{\min}}^{\Delta f_{\max}} d\Delta f \int_{\Delta f}^{\infty} df B(f, \Delta f)}{\left[2\int_{\Delta f_{\min}}^{\Delta f_{\max}} d\Delta f \int_{\Delta f}^{\infty} df E(f+\Delta f)E(f) \int_{\Delta f_{\min}}^{\Delta f_{\max}} d\Delta f E(\Delta f)\right]^{1/2}}. \tag{9}$$

Substitution of the theoretical expression for B, Eq. (A11) in Eq. (9), and again neglecting primary waves with frequency Δf, yields

$$\frac{\int_{\Delta f_{\min}}^{\Delta f_{\max}} d\Delta f E_{\text{forced}}(\Delta f)}{\int_{\Delta f_{\min}}^{\Delta f_{\max}} d\Delta f E(\Delta f)} = \alpha_{ii}|b_{ii}|^2, \qquad (10)$$

where α_{ii} is given by

$$\alpha_{ii} = \frac{N_2}{N_1^2} \qquad (11)$$

with

$$N_n = \frac{\int_{\Delta f_{\min}}^{\Delta f_{\max}} d\Delta f \int_{\Delta f}^{\infty} df \int_0^{2\pi} d\theta_1 \int_0^{2\pi} d\theta_2 D^n(f+\Delta f, -f, \Delta\theta+\pi)\, E(f+\Delta f, \theta_1)E(f, \theta_2)}{\int_{\Delta f_{\min}}^{\Delta f_{\max}} d\Delta f \int_{\Delta f}^{\infty} df \int_0^{2\pi} d\theta_1 \int_0^{2\pi} d\theta_2 E(f+\Delta f, \theta_1)E(f, \theta_2)}. \qquad (12)$$

Equations (10)–(12) show that $|b_{ii}|^2$ is approximately the fraction of energy in the frequency range $[\Delta f_{\min}, \Delta f_{\max}]$ that is locally nonlinearly forced (with a small negative bias, $\alpha_{ii} > 1$, discussed in section 5).

As shown in Fig. 4d, estimates of forced wave energy in the infragravity band ($\Delta f_{\min} = 0.005$ Hz, $\Delta f_{\max} = 0.05$ Hz) based on Eqs. (2), (9), and (10) (setting $\alpha_{ii} = 1$) are in excellent agreement with theoretical predictions, Eq. (1), even when forced waves contribute less than 1% of the total infragravity energy (Fig. 4b). The observed phases of b_{ii} (Fig. 5c) are generally within a few degrees of the theoretical value of 180° (i.e., imaginary part = 0). Overall, the bispectral analysis shows that the energy levels and phases of forced infragravity waves are accurately predicted by second-order nonlinear theory (Hasselmann 1962) for a wide range of conditions.

5. Discussion

Although there is general agreement between observed and predicted forced wave energy levels over a range of nearly 10^5 (Figs. 4c,d), discrepancies in individual frequency bands $[E_{\text{forced}}(\Delta f)]$ are sometimes as much as a factor of 50 (i.e., Figs. 3c and 4c), and the predicted and observed total forced wave energies differ by as much as a factor of 2 (differences of 30% are more typical, Fig. 4d). Errors in forced wave energy predictions, Eq. (1), are caused by inaccuracies in the swell–sea frequency–directional spectrum $E(f, \theta)$ estimated from finite length data records and a limited number of sensors. The variational technique (Herbers and Guza 1990) used here minimizes a roughness norm of $E(f, \theta)$ and generally results in an estimate directionally broader than the true $E(f, \theta)$. Owing to the decrease in the interaction coefficient D with increasing $\Delta\theta$ (Fig. 2), the resulting forced wave predictions $E_{\text{forced}}(\Delta f)$ [Eq. (1)] are expected to be biased low. Model tests indicate that this bias is less than 40%. The observed (based on bispectral analysis) forced wave energies and energy densities are also biased low because α_{ii}, $\alpha_i(\Delta f) > 1$ [Eqs. (7), (11)], rather than equal to 1 as assumed in all the results presented here. Using the estimated $E(f, \theta)$ to calculate $\alpha_i(\Delta f)$ and α_{ii} indicates that the observed $E_{\text{forced}}(\Delta f)$ and $\int d\Delta f E_{\text{forced}}(\Delta f)$ are biased low by about 20%–50% of the true value. Neither of these biases can explain the much larger scatter with low forced wave energy in Fig. 4c. Statistical uncertainty in the bispectral estimates is probably the dominant source of errors. Although statistics of bispectra are not well understood, numerical simulations for simple nonlinear processes (Elgar and Sebert 1989) indicate that the statistical uncertainty in bispectral estimates is relatively large when the nonlinearity is weak. Thus, when free waves dominate the infragravity spectrum ($|b_i(\Delta f)|^2 \ll 1$) estimates of $E_{\text{forced}}(\Delta f)$ based on Eq. (6) are expected to be inaccurate. The statistical uncertainty in bispectra is dramatically reduced by integration (cf. the relative size of imaginary parts in Figs. 5a–c), and (bispectrum-based) estimates of the total forced wave energy $[\int d\Delta f E_{\text{forced}}(\Delta f)]$ are considerably closer to the predicted values than estimates at individual frequencies $[E_{\text{forced}}(\Delta f)]$ (cf. Figs. 4c and 4d).

Although the observed forced wave energy (Fig. 4c,d) and phases (Fig. 5) are well predicted by second-order nonlinear theory (Hasselmann 1962), forced waves account for only a small part (0.07% to 30%) of the total observed infragravity energy. The forced fraction increases dramatically with increasing infragravity energy (Fig. 4b) as in Okihiro et al. (1992) and Elgar et al. (1992). Wavenumber estimates (to be discussed elsewhere) indicate that the infragravity energy that is not locally forced is contributed by free waves generated close to shore.

The mix of free and forced infragravity energy observed on the inner North Carolina shelf in 13 m depth is not necessarily representative of other sites. Whereas

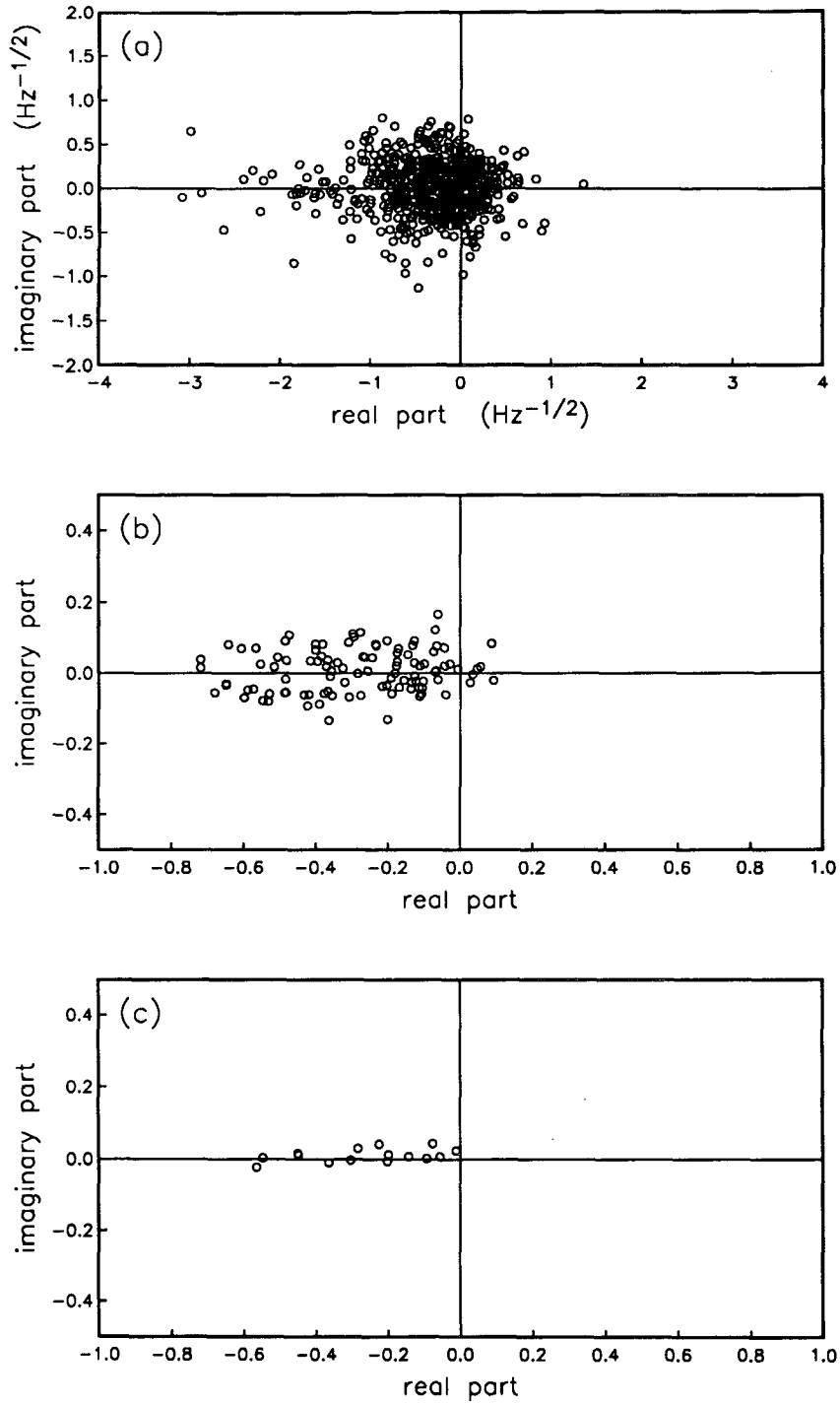

FIG. 5. Imaginary versus real parts of observed bispectra for all 15 runs: (a) $b(f_1, f_2)$ [Eq. (4)] for $f_1, f_1 + f_2$ in the range 0.06–0.24 Hz and the difference frequency f_2 in the range 0.005–0.05 Hz. (b) The single integral $b_i(\Delta f)$ [Eq. (5)] for Δf in the range 0.005–0.05 Hz. (c) The double integral b_{ii} [Eq. (9)] with $\Delta f_{min} = 0.005$ Hz and $\Delta f_{max} = 0.05$ Hz.

forced wave energy levels depend only on the local water depth and the swell–sea frequency–directional spectrum, free wave energy may also be a function of the surrounding shelf and beach topography. In Part 2 of this study, the variability of free infragravity energy will be investigated using long-term bottom pressure

measurements collected at many coastal locations in the Atlantic and Pacific Oceans, in depths ranging from 8 to 200 m, near islands and straight coastlines, and offshore of both steep and gently sloping beaches. The majority of these observations are single-point measurements, and estimates of $E(f, \theta)$ needed for theoretical predictions of forced wave energy [Eq. (1)] are unavailable. However, as shown here (Fig. 4c,d) the mix of forced and free infragravity energy can be estimated at least qualitatively well from single-point pressure measurements using integrals of the bispectrum, and this methodology will be used in Part 2.

Acknowledgments. This research was sponsored by the Office of Naval Research (the Geology and Geophysics and Coastal Sciences Programs, and the Nonlinear Ocean Waves Accelerated Research Initiative). The pressure sensor array was deployed and maintained by the staff of the Center for Coastal Studies, Scripps Institution of Oceanography. Excellent logistics support was provided by the U.S. Army Corps of Engineers Field Research Facility, Coastal Engineering Research Center, Duck, North Carolina.

APPENDIX

Spectra and Bispectra of Seafloor Pressure

The bottom pressure field $p(\mathbf{x}, t)$ of weakly nonlinear surface gravity waves in arbitrary water depth h can be derived through a perturbation expansion of the surface boundary conditions and Bernoulli equation (Hasselmann 1962; Hasselmann et al. 1963)

$$p(\mathbf{x}, t) = p^{(1)}(\mathbf{x}, t) + p^{(2)}(\mathbf{x}, t) + \cdots, \quad \text{(A1)}$$

where t denotes time and $\mathbf{x} = (x, y)$ is the horizontal space coordinate.

The primary bottom pressure field $p^{(1)}(\mathbf{x}, t)$ can be expressed as the Fourier–Stieltjes transform (Hasselmann 1962)

$$p^{(1)}(\mathbf{x}, t) = \int_{\mathbf{k}} \exp[i\mathbf{k}\cdot\mathbf{x}][dP_{-}^{(1)}(\mathbf{k}) \exp[i2\pi ft] + dP_{+}^{(1)}(\mathbf{k}) \exp[-i2\pi ft]], \quad \text{(A2)}$$

where $\mathbf{k}$ is the vector wavenumber [$\mathbf{k} = (k\cos\theta, k\sin\theta)$, with θ the propagation direction], $dP_{-}^{(1)}(\mathbf{k})$ is the complex conjugate of $dP_{+}^{(1)}(-\mathbf{k})$, and f is given by the dispersion relation

$$f = \frac{1}{2\pi}[gk \tanh(kh)]^{1/2}, \quad \text{(A3)}$$

where g is the acceleration of gravity. The secondary bottom pressure field $p^{(2)}(\mathbf{x}, t)$ is given by

$$p^{(2)}(\mathbf{x}, t) = \int_{\mathbf{k}_1}\int_{\mathbf{k}_2} \exp[i(\mathbf{k}_1 + \mathbf{k}_2)\cdot\mathbf{x}] \times \sum_{s_1, s_2 = \pm 1} \mathrm{D}(s_1 f_1, s_2 f_2, \Delta\theta) dP_{s_1}^{(1)}(\mathbf{k}_1) dP_{s_2}^{(1)}(\mathbf{k}_2) \times \exp[-i2\pi(s_1 f_1 + s_2 f_2)t], \quad \text{(A4)}$$

where $\Delta\theta = \theta_1 - \theta_2$ is the difference in propagation directions of the interacting pair of primary wave components $(s_1 f_1, \mathbf{k}_1)$ and $(s_2 f_2, \mathbf{k}_2)$ [with directions θ_1 and θ_2, $\mathbf{k}_i = (k_i\cos\theta_i, k_i\sin\theta_i)$ and f_i, k_i related by the dispersion relation, Eq. (A3)] and D is the interaction coefficient

$$D(s_1 f_1, s_2 f_2, \Delta\theta) \equiv -\frac{gk_1k_2\cos(\Delta\theta)}{2\sigma_1\sigma_2} + \frac{g(\sigma_1 + \sigma_2)\cosh(k_1h)\cosh(k_2h)}{[gk_3\tanh(k_3h) - (\sigma_1 + \sigma_2)^2]\sigma_1\sigma_2\cosh(k_3h)} \times \left\{(\sigma_1 + \sigma_2)\left[\frac{(\sigma_1\sigma_2)^2}{g^2} - k_1k_2\cos(\Delta\theta)\right] - \frac{1}{2}\left[\frac{\sigma_1k_2^2}{\cosh^2(k_2h)} + \frac{\sigma_2k_1^2}{\cosh^2(k_1h)}\right]\right\}, \quad \text{(A5)}$$

with $\sigma_i \equiv 2\pi s_i f_i$ and $k_3 \equiv |\mathbf{k}_1 + \mathbf{k}_2| = [k_1^2 + k_2^2 + k_1k_2\cos(\Delta\theta)]^{1/2}$.

Hasselmann's weakly nonlinear theory is formally valid only for the irrotational wave motion above the wave bottom boundary layer, whereas the pressure transducers (buried about 10 cm in the sand) measure pressure below the boundary layer. Turbulent boundary-layer effects on secondary wave pressure at the seafloor are not understood but are expected to be small if the contribution of the local flow $\mathbf{u}$ (the Bernoulli pressure $-|\mathbf{u}|^2/2g$) to the secondary bottom pressure field is small. The relative contribution of the Bernoulli term [the first term on the right-hand side of Eq. (A5)] to $p^{(2)}$ is O(20%) for the dominant nonlinear interactions in the present observations. Pressure changes across the wave bottom boundary layer are neglected.

The spectrum of forced secondary waves

$$E_{\text{forced}}(f) \equiv 2\int_{-\infty}^{\infty} d\tau \times \mathbf{E}\{p^{(2)}(t)p^{(2)}(t + \tau)\} \exp[-i2\pi f\tau], \quad \text{(A6)}$$

where $\mathbf{E}\{\ \}$ denotes the expected value, can be expressed in terms of the frequency-directional spectrum of primary waves

$$E(f, \theta)dfd\theta \equiv 2\mathbf{E}\{dP_{+}^{(1)}(\mathbf{k})dP_{-}^{(1)}(-\mathbf{k})\} \quad \text{(A7)}$$

and the interaction coefficient D

$$E_{\text{forced}}(f) = \int_0^f df' \int_0^{2\pi} d\theta_1 \int_0^{2\pi} d\theta_2 \times D^2(f - f', f', \Delta\theta)E(f - f', \theta_1)E(f', \theta_2) + 2\int_0^{\infty} df' \int_0^{2\pi} d\theta_1 \int_0^{2\pi} d\theta_2 D^2(f + f', -f', \Delta\theta + \pi)E(f + f', \theta_1)E(f', \theta_2). \quad \text{(A8)}$$

The first and second terms on the right-hand side of Eq. (A8) result from sum-frequency [$s_1 = s_2$ in Eq.

(A4)] and difference-frequency [$s_1 = -s_2$ in Eq. (A4)] interactions, respectively.

Analogous to the conventional energy-density spectrum, Hasselmann et al. (1963) introduced the bispectrum $B(f_1, f_2)$

$$B(f_1, f_2) \equiv 2 \int_{-\infty}^{\infty} d\tau_1 \int_{-\infty}^{\infty} d\tau_2 R(\tau_1, \tau_2) \times \exp[-2\pi i(f_1\tau_1 + f_2\tau_2)], \quad \text{(A9)}$$

where $R(\tau_1, \tau_2)$ is the third-order correlation function

$$R(\tau_1, \tau_2) \equiv \mathbf{E}\{p(t)p(t+\tau_1)p(t+\tau_2)\} \quad \text{(A10)}$$

[Eq. (2b) is an alternate but equivalent definition of $B(f_1, f_2)$]. Substitution of Eqs. (A1), (A2), (A4), and (A7) in Eqs. (A9) and (A10) yields the lowest-order contribution to the bispectrum (Hasselmann et al. 1963):

$$\begin{aligned} B(f_1, f_2) = \int_0^{2\pi} d\theta_1 \int_0^{2\pi} d\theta_2 [& D(f_1, f_2, \Delta\theta) E(f_1, \theta_1) \\ & \times E(f_2, \theta_2) + D(f_1 + f_2, -f_2, \Delta\theta + \pi) \\ & \times E(f_1 + f_2, \theta_1) E(f_2, \theta_2) \\ & + D(-f_1, f_1 + f_2, \Delta\theta + \pi) \\ & \times E(f_1, \theta_1) E(f_1 + f_2, \theta_2)]. \end{aligned} \quad \text{(A11)}$$

The first, second, and third terms on the right-hand side of Eq. (A11) result from sum interactions of waves with frequencies f_1 and f_2, difference interactions of waves with frequencies f_2 and $f_1 + f_2$, and difference interactions of waves with frequencies f_1 and $f_1 + f_2$, respectively.

REFERENCES

Birkemeier, W., K. Hathaway, J. Smith, C. Baron, and M. Leffler, 1991: DELILAH Experiment: Investigator's summary report. U.S. Army Corps of Engineers. 12 pp.

Bowen, A. J., and R. T. Guza, 1978: Edge waves and surf beat. *J. Geophys. Res.*, **83,** 1913–1920.

Elgar, S., and R. T. Guza, 1985: Observations of bispectra of shoaling surface gravity waves. *J. Fluid Mech.*, **161,** 425–448.

——, and G. Sebert, 1989: Statistics of bicoherence and biphase. *J. Geophys. Res.*, **94,** 10 993–10 998.

——, T. H. C. Herbers, M. Okihiro, J. Oltman-Shay, and R. T. Guza, 1992: Observations of infragravity waves. *J. Geophys. Res.*, **97,** 15 573–15 577.

Foda, M. A., and C. C. Mei, 1981: Nonlinear excitation of long-trapped waves by a group of short swells. *J. Fluid Mech.*, **111,** 319–345.

Gallagher, B., 1971: Generation of surf beat by non-linear wave interactions. *J. Fluid Mech.*, **49,** 1–20.

Guza, R. T., and E. B. Thornton, 1985: Observations of surf beat. *J. Geophys. Res.*, **90,** 3161–3172.

Hasselmann, K., 1962: On the non-linear energy transfer in a gravity-wave spectrum. Part 1: General theory. *J. Fluid Mech.*, **12,** 481–500.

——, W. Munk, and G. MacDonald, 1963: Bispectra of ocean waves. *Times Series Analysis,* M. Rosenblatt, Ed., John Wiley, 125–139.

Haubrich, R. A., 1965: Earth noise, 5 to 500 millicycles per second. 1. Spectral stationarity, normality, and nonlinearity. *J. Geophys. Res.*, **70,** 1415–1427.

Herbers, T. H. C., and R. T. Guza, 1990: Estimation of directional wave spectra from multicomponent observations. *J. Phys. Oceanogr.*, **20,** 1703–1724.

——, and ——, 1994: Nonlinear wave interactions and high-frequency sea floor pressure. *J. Geophys. Res.*, in press.

Holman, R. A., D. A. Huntley, and A. J. Bowen, 1978: Infragravity waves in storm conditions. *Proc. 16th Conf. on Coastal Engineering,* American Society of Civil Engineers, 268–284.

Howd, P. J., J. Oltman-Shay, and R. A. Holman, 1991: Wave variance partitioning in the trough of a barred beach. *J. Geophys. Res.*, **96,** 12 781–12 795.

Huntley, D. A., R. T. Guza, and E. B. Thornton, 1981: Field observations of surf beat. Part 1: Progressive edge waves. *J. Geophys. Res.*, **86,** 6451–6466.

List, J. H., 1992: A model for the generation of two-dimensional surf beat. *J. Geophys. Res.*, **97,** 5623–5636.

Longuet-Higgins, M. S., and R. W. Stewart, 1962: Radiation stress and mass transport in surface gravity waves with application to "surf beats." *J. Fluid Mech.*, **13,** 481–504.

Mei, C. C., and C. Benmoussa, 1984: Long waves induced by short-wave groups over an uneven bottom. *J. Fluid Mech.*, **139,** 219–235.

Munk, W. H., 1949: Surf beats. *Eos, Trans. Amer. Geophys. Union,* **30,** 849–854.

——, F. Snodgrass, and F. Gilbert, 1964: Long waves on the continental shelf: An experiment to separate trapped and leaky modes. *J. Fluid Mech.*, **20,** 529–554.

Okihiro, M., R. T. Guza, and R. J. Seymour, 1992: Bound infragravity waves. *J. Geophys. Res.*, **97,** 11 453–11 469.

Oltman-Shay, J., and R. T. Guza, 1987: Infragravity edge wave observations on two California beaches. *J. Phys. Oceanogr.*, **17,** 644–663.

Sand, S. E., 1982: Wave grouping described by bounded long waves. *Ocean Eng.*, **9**(6), 567–580.

Schäffer, H. A., and I. A. Svendsen, 1988: Surf beat generation on a mild slope beach. *Proc. 21st Conf. on Coastal Engineering,* American Society of Civil Engineers, 1058–1072.

——, I. G. Jonsson, and I. A. Svendsen, 1990: Free and forced cross-shore long waves. *Water Wave Kinematics,* A. Torum and O. T. Gudmestad, Eds., Kluwer Academic, 367–385.

Symonds, G., D. A. Huntley, and A. J. Bowen, 1982: Two-dimensional surf beat: Long wave generation by a time-varying breakpoint. *J. Geophys. Res.*, **87,** 492–498.

Tucker, M. J., 1950: Surf beats: Sea waves of 1 to 5 minute period. *Proc. Roy. Soc. London,* **A202,** 565–573.

Webb, S. C., X. Zhang, and W. Crawford, 1991: Infragravity waves in the deep ocean. *J. Geophys. Res.*, **96,** 2723–2736.

Wright, L. D., R. T. Guza, and A. D. Short, 1982: Dynamics of a high-energy dissipative surf zone. *Mar. Geol.*, **45,** 41–62.